DØ Note 5882-CONF

Search for $t\bar{t}$ Resonances in the Lepton+Jets Final State in $p\bar{p}$ Collisions at $\sqrt{s} = 1.96\,\text{TeV}$

The DØ Collaboration
URL http://www-d0.fnal.gov
(Dated: March 16, 2009)

A search for a narrow-width heavy resonance decaying into top quark pairs ($X \to t\bar{t}$) in $p\bar{p}$ collisions at a center of mass energy $\sqrt{s} = 1.96\,\text{TeV}$ has been performed using data collected with the DØ detector at the Fermilab Tevatron Collider. This analysis considers $t\bar{t}$ candidate events in the lepton+jets channel using a neural network to identify b-jets and the $t\bar{t}$ invariant mass distribution to search for evidence of resonant production. The analyzed dataset corresponds to an integrated luminosity of approximately $3.6\,\text{fb}^{-1}$. We find no evidence for a narrow resonance X decaying to $t\bar{t}$. Therefore, we set upper limits on cross section times branching ratio $\sigma_X \cdot B(X \to t\bar{t})$ for different hypothesized resonance masses using a Bayesian approach. Within a topcolor-assisted technicolor model, the existence of a leptophobic Z' boson with mass $M_{Z'} < 820\,\text{GeV}$ and width $\Gamma_{Z'} = 0.012 M_{Z'}$ can be excluded at 95% C.L.

Preliminary Result for Winter 2009 Conferences

I. INTRODUCTION

The top quark has by far the largest mass of all the known fermions. Heavy, yet unknown resonances may play a role in the production of top pairs and add a resonant part to the Standard Model mechanism. Such resonant production is possible for massive Z-like bosons in extended gauge theories [1], Kaluza Klein states of the gluon or Z boson [2, 3], axigluons [4], topcolor [5], and other theories beyond the Standard Model. Independent of the exact model, a narrow width resonance should be visible in the $t\bar{t}$ invariant mass distribution. A wide resonance will be very hard to observe in the $t\bar{t}$ spectrum.

In this note a search for a narrow-width heavy resonance X decaying into $t\bar{t}$ is presented. We consider the lepton+jets (ℓ+jets, where $\ell = e$ or μ) final state. The event signature is one isolated electron or muon with high transverse momentum (p_T), large transverse energy imbalance ($\not\!\!E_T$) due to the undetected neutrino, and at least three jets, two of which result from the hadronization of b quarks. The analyzed D0 data set includes about $1.0\,\mathrm{fb}^{-1}$ from Tevatron Run IIa (August 2002 to December 2005) and about $2.6\,\mathrm{fb}^{-1}$ from Run IIb (January 2006 to July 2008). The signal to background ratio is improved by identifying b-jets using a neural network based b-tagging algorithm. After b-tagging, the dominant physics background for a resonance signal is non-resonant SM $t\bar{t}$ production. Smaller contributions arise from the direct production of W bosons in association with three or more jets (W+jets), as well as instrumental background originating from multijet processes with jets faking isolated leptons. The distribution of the events total invariant mass observed in data is compared to templates for the expected SM backgrounds and narrow resonance signals of various masses. No excess is observed above backgrounds. Limits obtained on $\sigma_X \cdot B(X \to t\bar{t})$ are used to set a lower bound on the mass, using a Bayesian method.

Previous searches performed by CDF and D0 in Run I and Run II found no evidence for a $t\bar{t}$ resonance [6–11]. In these studies a top-color model was used as a reference for quoting mass limits. A large top quark mass can be generated through the formation of a dynamical $t\bar{t}$ condensate, X, due to a new strong gauge force coupling preferentially to the third generation of fermions [5]. In one particular model, top-color-assisted technicolor [12], the Z' boson couples weakly and symmetrically to the first and second generations but strongly to the third generation of quarks, and has no couplings to leptons. Thus the SM $q\bar{q}$ annihilation process is augmented by a resonance contribution from Z' decay. Recent results yield $M_{Z'} > 760$ GeV for the DØ analysis [10] and $M_{Z'} > 725$ GeV for the CDF analysis [8, 9], both for a resonance with $\Gamma_{Z'} = 0.012 M_{Z'}$.

II. DØ DETECTOR

The D0 detector [13] has a central-tracking system consisting of a silicon microstrip tracker and a central fiber tracker, both located within a 2 T superconducting solenoidal magnet, with designs optimized for tracking and vertexing at pseudorapidities $|\eta| < 3$ and $|\eta| < 2.5$ respectively. Central and forward preshower detectors are positioned just outside of the superconducting coil. A liquid-argon and uranium calorimeter has a central section (CC) covering pseudorapidities $|\eta|$ up to ≈ 1.1, and two end calorimeters (EC) that extend coverage to $|\eta| \approx 4.2$, with all three housed in separate cryostats [14]. An outer muon system, at $|\eta| < 2$, consists of a layer of tracking detectors and scintillation trigger counters in front of 1.8 T toroids, followed by two similar layers after the toroids [15]. Luminosity is measured using plastic scintillator arrays placed in front of the EC cryostats. The trigger and data acquisition systems are designed to accommodate the high luminosities of Run II.

III. EVENT SELECTION

To select top pair events in the e+jets and μ+jets decay channels, triggers that required a jet and an electron or muon are used. Offline we require either an isolated electron with $p_T > 20\,\mathrm{GeV}$ and $|\eta| < 1.1$, or an isolated muon with $p_T > 25\,\mathrm{GeV}$ and $|\eta| < 2.0$. No additional isolated leptons with $p_T > 15\,\mathrm{GeV}$ are allowed in the event [16, 17]. Jets are defined using a cone algorithm [18] with radius $R_{cone} = 0.5$, where $R_{cone} = \sqrt{(\Delta\phi)^2 + (\Delta y)^2}$, ϕ is the azimuthal angle, and y is the rapidity. The selected events must contain three or more jets with $p_T > 20\,\mathrm{GeV}$ and $|\eta| < 2.5$. At least one of the jets is required to have $p_T > 40\,\mathrm{GeV}$. We require $\not\!\!E_T$ to exceed 20 GeV (25 GeV) for the e+jets (μ+jets) channel and to not be collinear with the lepton direction in the transverse plane. In the muon+jets channel, events with a mismeasured muon momentum are rejected by requiring $\Delta\phi(\mu, \not\!\!E_T) > 2.1 - 0.035\,\not\!\!E_T\,(\mathrm{GeV})$, where $\Delta\phi(\mu, \not\!\!E_T)$ denotes the azimuthal angle, in radians, between the muon and $\not\!\!E_T$ directions, and $\not\!\!E_T$ is in GeV. Events where a second muon gives an invariant mass of the two muons within 70 to 100 GeV are rejected. In the electron+jets channel, events with a mismeasured electron momentum are rejected by requiring $\Delta\phi(e, \not\!\!E_T) > 2.2 - 0.045\,\not\!\!E_T\,(\mathrm{GeV})$.

In order to improve the signal to background ratio, at least one jet is required to be identified as a b-jet. The tagging algorithm uses the impact parameters of tracks matched to a given jet, information on vertex mass, the significance

of displacement, and the number of participating tracks for any reconstructed secondary vertex within the cone of the given jet. The output variable, NN_B, is near one for b-jets and near zero for light jets [19]. In this analysis we consider jets as b-tagged if $\mathrm{NN}_B > 0.65$ which corresponds to a tagging efficiency for b-jets of about 55% at a rate for light partons (u, d, s, g) of less than 1%. We independently analyze singly b-tagged and doubly b-tagged events since the channels have different systematic uncertainties.

IV. SIGNAL AND BACKGROUND MODELING

Simulated events are used to determine selection efficiencies for the resonant $t\bar{t}$ production signal and for background sources except those in which instrumental effects give fake leptons and $\not\!\!E_T$ in multijet production events. Samples of resonant $t\bar{t}$ production are generated with PYTHIA [20] for ten different choices of the resonance mass M_X between 350 GeV and 1.0 TeV and width of the resonance of $\Gamma_X = 0.012 M_X$. This qualifies the X boson as a narrow resonance since its width is smaller than the mass resolution of the DØ detector. Resonances with Z-like, vector, and axial vector couplings have been produced. The generated resonances are forced to decay into $t\bar{t}$.

The standard model $t\bar{t}$ process is generated with ALPGEN [21] plus PYTHIA for fragmentation using a top quark mass of 172.5 GeV (175 GeV) for Run IIb (RunIIa). We use the MLM [22] jet matching algorithm to avoid double counting of radiation from the hard matrix element and the parton shower. Similarly, W+jets and Z+jets events are generated using ALPGEN plus PYTHIA. Diboson backgrounds (WW, WZ and ZZ) are generated with PYTHIA. The single top quark production is generated using the COMPHEP generator [23]. For all samples the PDF set CTEQ6L1 [24] is employed. The generated events are processed through the full GEANT3-based [25] D0 detector simulation and the same reconstruction program used for data.

The MC-generated SM backgrounds are used both to obtain the total acceptance and the shape of the reconstructed $t\bar{t}$ invariant mass distribution. Trigger and reconstruction inefficiencies are accounted for by weighting the simulated events. Jet b-tagging probabilities are measured in data and parametrized as function of p_T and η depending on the simulated flavor. They are used to weight each simulated event according to its event b-tagging probability.

We use the $t\bar{t}$ production cross-section $\sigma_{t\bar{t}}(m_t = 172.4\,\mathrm{GeV}) = 7.48\,\mathrm{pb}$ [26] for normalization. Single top and diboson samples are normalized to their NLO cross-sections [27, 28]. For Z+jets the LO generator cross-sections are corrected to NLO using K-factors of 1.30 for Z+light partons, 1.52 for $Z + b\bar{b}$, and 1.67 for $Z + c\bar{c}$.

The combined acceptance times efficiency times branching fractions for SM $t\bar{t}$ production is 3.4% (4.4%) for the 3 jet (≥ 4 jet) samples. The corresponding numbers for a 650 GeV topcolor Z' resonance with $B(Z' \to t\bar{t}) = 1$ are 2.8% (3.9%).

The W+jets background is estimated from a combination of data and MC information. The expected number of W+jets events in the b-tagged sample is computed as the product of the estimated number of W+jets before b-tagging and the expected event b-tagging probability. The former is obtained from the observed number of events with real leptons in data, computed using the Matrix Method [16], and then subtracting the expected contributions from other SM production processes. The b-tagging probability is obtained by combining the W+jets flavor fractions estimated from MC with the event b-tagging probability, estimated from b-tag rate functions. The fraction of heavy flavor in the W+jets background has been measured in control samples and a corresponding uncertainty on the W+jets flavor composition is determined. The shape of the reconstructed invariant mass distribution is obtained from the MC simulation.

The multijet background is determined from data. The total number of expected events is estimated by applying the Matrix Method on the b-tagged sample. The shape is derived from events with leptons failing the isolation requirements.

V. RECONSTRUCTION OF THE $t\bar{t}$ INVARIANT MASS DISTRIBUTION

The $t\bar{t}$ invariant mass is reconstructed from the four-momenta of up to four leading jets, the lepton momentum and the neutrino momentum. The latter is obtained from the transverse missing energy, $\not\!\!E_T$, and by solving $M_W^2 = (p^l + p^\nu)^2$ for the component of the neutrino momentum along the beam direction, using $\not\!\!E_T$ for the neutrino transverse momentum. If there are two real solutions, the one with the smaller $|p_z^\nu|$ is taken; if no real solution exists, p_z^ν is set to 0. This method was shown to give better sensitivity for high mass resonances than a previously applied constrained kinematic fit technique [7], while only slightly reducing the sensitivity for lower resonance masses. Moreover, this direct reconstruction allows the inclusion of data with fewer than four jets in the case that some jets are merged, further increasing the sensitivity. The shapes of the invariant mass distributions expected for three different resonance masses are compared with that for the SM $t\bar{t}$ production in Fig. 1.

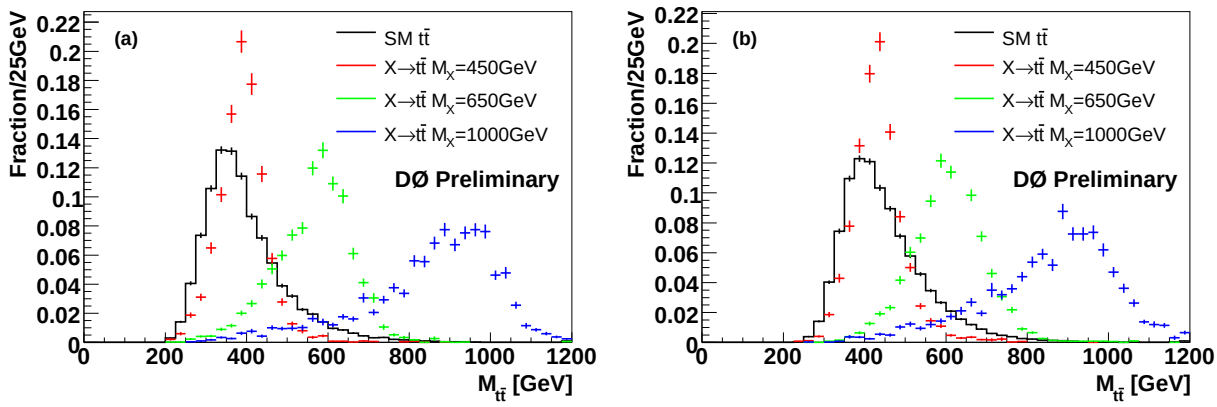

FIG. 1: Shape comparison of expected $t\bar{t}$ invariant mass distribution for Run IIa data set for standard model top pair production (histogram) compared to resonant production from narrow-width resonances of mass $M_X = 450$, 650 GeV, and $M_X = 1$ TeV, for (a) 3 jet events and (b) ≥ 4 jet events.

VI. SYSTEMATIC UNCERTAINTIES

The systematic uncertainties can be classified as those affecting only normalization and those affecting the shape of any of the signal or background invariant mass distribution. The systematic uncertainties affecting only the normalization include the theoretical uncertainty on the SM prediction for $\sigma_{t\bar{t}}$, the uncertainty on the integrated luminosity (6.1%) [29] and the uncertainty of lepton identification efficiencies.

The systematic uncertainties affecting the shape of the invariant mass distribution as well as the normalization have been determined for both signal and background samples. These include uncertainties on the jet energy calibration, the jet reconstruction efficiency and b-tagging parametrizations for b, c and light quark jets. The central $t\bar{t}$ cross-section of 7.48 pb, appropriate for $m_t = 172.4$ GeV, is taken with an uncertainty of $^{+0.56}_{-0.72}$ pb [30] to obtain the systematic uncertainty on the $t\bar{t}$ background normalization. This includes the cross section variation due to a top mass uncertainty of ± 1.2 GeV [31]. The kinematic changes due to top mass uncertainty are evaluated by replacing the default SM background simulation with simulation done at top quark masses of 170 and 180 GeV (170 and 175 GeV) for RunIIa (RunIIb) and taking half this variation to obtain the 1σ errors for each of the two samples, corresponding getting to a top mass uncertainty of 2.5 GeV (1.25 GeV) for RunIIa (RunIIb). Also the uncertainties of tuning the parameterization of the b-fragmentation function, the determination of the heavy flavor fraction in W+jets, and the uncertainties of the efficiencies used in the Matrix Method were propagated to the limit setting.

Tables III and IV give a summary of the relative systematic uncertainties on the total SM background normalization for the combined ℓ+jets channels in Run II. The effect of the different systematic uncertainties on the shape of the $t\bar{t}$ invariant mass distribution can not be inferred from this table.

VII. RESULT

After all selection cuts 1293 events remain in the e+jets channel and 1052 events in the μ+jets channel. The sums of all standard model and multijet instrumental backgrounds are 1329 ± 36 and 1053 ± 32 events, respectively. The event

	3 jets	≥ 4 jets
$t\bar{t}$	624	721
Single top	47	13
Diboson	32	8
W+jets	592	129
Z+jets	85	26
Multijet	84	22
Total background	1464	919
Data	1411	934

TABLE I: Event yields from data and for the SM expectation.

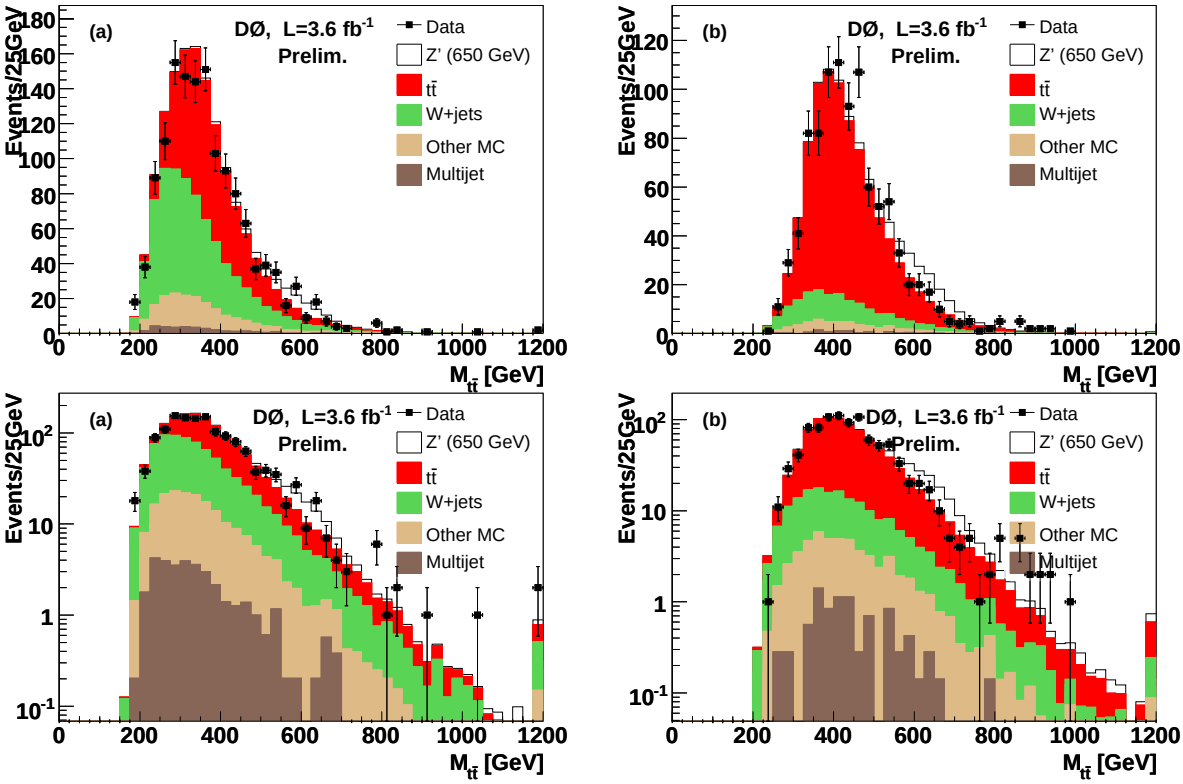

FIG. 2: Expected and observed $t\bar{t}$ invariant mass distribution for the combined $\ell + 3$jets, and $\ell + 4$ or more jets channels, with at least one identified b-jet. The error bars for the data drawn on top of the SM background indicate the statistical uncertainty. Superimposed as white area is the theory signal for a top-color-assisted technicolor Z' boson with $M_{Z'} = 650\,\text{GeV}$. The number of data, signal and expected background events from each source are indicated in Table I.

yields for the data and background sources are indicated in Table I. Invariant mass distributions are computed for events with exactly one b-tag and for events with more than one b-tag. Additionally, the distributions are separated into 3 jet and 4 or more jet samples, as well as Run IIa and Run IIb data ranges. The measured invariant mass distributions and corresponding background estimations are shown in Fig. 2 for the 3 and ≥ 4 jet samples for Run IIa and Run IIb samples combined.

Finding no significant deviation from the standard model expectation, a Bayesian approach is applied to calculate 95% C.L. upper limits on $\sigma_X \cdot B(X \to t\bar{t})$ for hypothesized values of M_X between 350 and 1000 GeV. A Poisson distribution is assumed for the number of observed events in each bin, and flat prior probabilities are taken for the signal cross-section times branching fraction. The prior for the combined signal acceptance and background yields is a multivariate Gaussian with uncertainties and correlations described by a covariance matrix [32].

The expected and observed 95% C.L. upper limits on $\sigma_X \cdot B(X \to t\bar{t})$ as a function of M_X, after combining the 1 and 2 b-tag samples and the 3 and $\geq$4 jet samples, are summarized in Table II and displayed in Fig. 3. Figure 3 also shows the theoretical prediction [5] for the topcolor Z' resonance production. The 95% C.L. lower Z' mass limit is derived by intersecting the theory prediction with the expected (observed) 95% C.L. lower limit on $\sigma_X \cdot B(X \to t\bar{t})$. The expected limit for the Z' boson is 870 GeV. The full Run II dataset used in this analysis excludes a Z' boson with masses $M_{Z'} < 820\,\text{GeV}$. The limits for the Run IIa (Run IIb) subsamples individually are 685 (820) GeV.

Figure 4 shows the measured $\sigma_X \cdot B(X \to t\bar{t})$ values as a function of M_X, together wtih the expected exclusion region. The small excess of events around $M_X \approx 650$ GeV seen in Fig. 2 gives rise to an observed resonance cross section of less than 2σ significance.

The limits for pure vector or pure axial vector couplings of the Z' to top quark pairs were compared for part of the Run IIb data set ($1.2\,\text{fb}^{-1}$). No difference was observed, therefore we conclude that our limit is valid for narrow resonances of any arbitrary vector and axial vector couplings.

M_X [GeV]	exp. limit [pb]	obs. limit [pb]
350	0.98	1.00
400	1.19	0.87
450	1.01	0.96
500	0.72	0.81
550	0.49	0.61
600	0.35	0.56
650	0.27	0.53
750	0.18	0.24
850	0.13	0.22
1000	0.10	0.16

TABLE II: Expected and observed limits for $\sigma_X \cdot B(X \to t\bar{t})$ at the 95% confidence level when combining all channels and taking all systematic uncertainties into account.

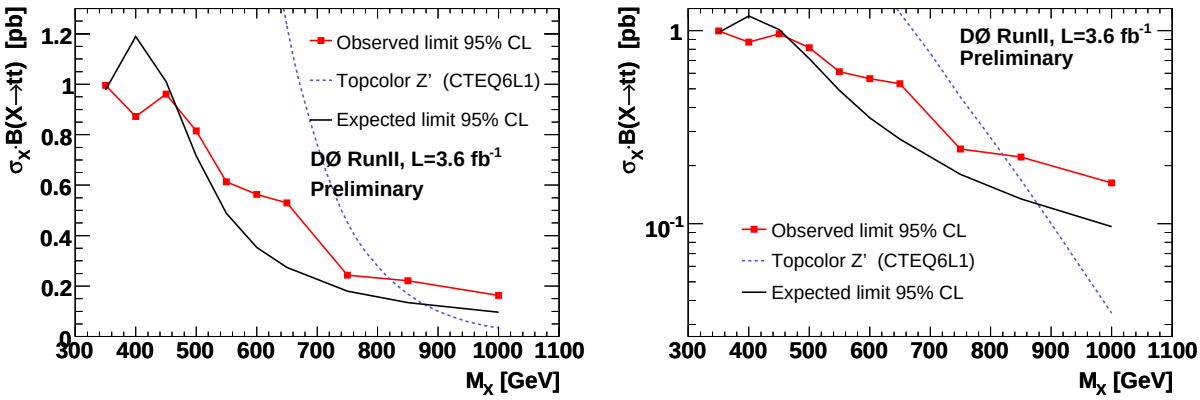

FIG. 3: Expected and observed $\sigma_X \cdot B(X \to t\bar{t})$ obtained in $3.6\,\mathrm{fb}^{-1}$ using Bayesian statistics. The black curve shows the 95% expected exclusion region, while the red curve with points shows the corresponding observed 95% C.L. upper limits. The theoretical prediction for a top-color-assisted technicolor Z' boson with a width of $\Gamma_{Z'} = 0.012 M_{Z'}$ as a function of the resonance mass M_X is shown as a dashed line.

VIII. CONCLUSION

A search for a narrow-width heavy resonance decaying to $t\bar{t}$ in the ℓ+jets final states has been performed using data corresponding to an integrated luminosity of about $3.6\,\mathrm{fb}^{-1}$, collected with the DØ detector at the Tevatron collider. By analyzing the reconstructed $t\bar{t}$ invariant mass distribution and using a Bayesian method, model independent upper limits on $\sigma_X \cdot B(X \to t\bar{t})$ have been obtained for different hypothesized masses of a narrow-width heavy resonance decaying into $t\bar{t}$. Within a top-color-assisted technicolor model, the existence of a leptophobic Z' boson with $M_{Z'} < 820\,\mathrm{GeV}$ and width around $\Gamma_{Z'} = 0.012 M_{Z'}$ is excluded at 95% C.L.

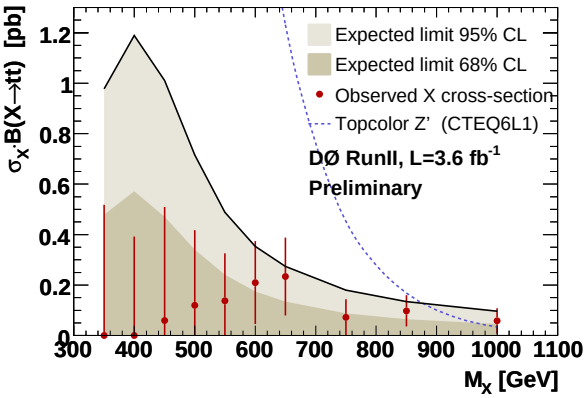

FIG. 4: The data points show the measured $\sigma_X \cdot B(X \to t\bar{t})$ for a narrow resonance obtained for the full data set, as a function of M_X. The shaded areas indicate 68% and 95% fluctuation bands expected under the assumption of pure SM $t\bar{t}$ production.

source	rel. sys. uncertainty (%) Standard Model processes				Resonance $M_X = 650\,\text{GeV}$			
	3 jets		≥4 jets		3 jets		≥4 jets	
	σ^+	σ^-	σ^+	σ^-	σ^+	σ^-	σ^+	σ^-
Jet energy calibration	−0.4	0.2	−0.2	−0.3	−2.0	1.3	3.2	−2.7
Jet energy resolution	−0.2	−0.1	−0.2	−0.2	−0.1	0.2	0.0	0.1
Jet identification	−0.4	0.4	−0.4	0.4	1.2	−1.2	−2.2	2.2
$\sigma_{t\bar{t}}(m_t = 170\,\text{GeV})$	2.3	−2.3	4.0	−4.0	–	–	–	–
W+jets (heavy flavor)	1.7	−1.6	0.7	−0.6	–	–	–	–
b fragmentation	0.1	–	0.1	–	0.8	–	1.3	–
Multijet lepton fake rate	0.6	−0.6	−0.2	0.1	–	–	–	–
Luminosity	2.6	−2.4	4.1	−3.8	6.0	−5.8	6.1	−5.8
Top quark mass	1.5	2.2	0.5	1.2	–	–	–	–
Selection efficiencies	1.8	−1.8	2.9	−2.9	3.6	−3.7	3.6	−3.6
b-tagging	3.1	−3.1	3.2	−3.3	3.9	−4.1	3.5	−3.7

TABLE III: Summary of the relative systematic change on the overall normalization in percent of the Standard Model background and for an resonance mass of $M_X = 650\,\text{GeV}$ with ≥ 1 b-tag for RunIIa. For all sources there are both normalization uncertainties which are shown here and mass-dependent shape uncertainties which are not shown, but are properly accounted for in setting limits.

source	rel. sys. uncertainty (%) Standard Model processes				Resonance $M_X = 650\,\text{GeV}$			
	3 jets		≥4 jets		3 jets		≥4 jets	
	σ^+	σ^-	σ^+	σ^-	σ^+	σ^-	σ^+	σ^-
Jet energy calibration	−1.2	1.3	2.8	−2.7	−1.7	1.1	3.6	−3.6
Jet energy resolution	−3.2	1.7	0.5	−0.6	−2.2	0.8	1.7	−1.1
Jet identification	0.1	−0.1	−1.2	1.2	0.2	−0.2	−1.6	1.6
$\sigma_{t\bar{t}}(m_t = 170\,\text{GeV})$	2.6	−3.3	4.8	−6.1	–	–	–	–
W+jets (heavy flavor)	1.0	0.0	0.4	−0.2	–	–	–	–
b fragmentation	−7.0	–	−6.0	–	−6.7	–	−6.1	–
Multijet lepton fake rate	−0.2	0.2	−0.1	0.1	–	–	–	–
Luminosity	2.1	−2.0	3.9	−3.7	6.1	−5.8	6.1	−5.8
Top quark mass	−1.0	1.2	−1.4	2.0	–	–	–	–
Selection efficiencies	1.4	−1.4	2.3	−2.3	3.6	−3.6	3.6	−3.6
b-tagging	5.4	−9.9	5.7	−8.7	7.2	−9.8	6.5	−8.9

TABLE IV: Summary of the relative systematic change on the overall normalization in percent of the Standard Model background and for an resonance mass of $M_X = 650\,\text{GeV}$ with ≥ 1 b-tags for RunIIb. For all sources there are both normalization uncertainties which are shown here and mass-dependent shape uncertainties which are not shown, but are properly accounted for in setting limits.

[1] A. Leike, "The phenomenology of extra neutral gauge bosons," Phys. Rept. 317 (1999) 143.
[2] B. Lillie, L. Randall, and L.-T. Wang, "The bulk RS KK-gluon at the LHC," JHEP 09 (2007) 074.
[3] T. G. Rizzo, "Testing the nature of kaluza-klein excitations at future lepton colliders," Phys. Rev. D 61 (2000) 055005.
[4] L. M. Sehgal and M. Wanninger, "Forward - backward asymmetry in two jet events: Signature of axigluons in proton - anti-proton collisions," Phys. Lett. B 200 (1988) 211.
[5] C. T. Hill and S. Parke, "Top production: sensitivity to new physics," Phys. Rev. D 49 (1994) 4454.
[6] CDF Collaboration, T. Affolder et al., "Search for new particles decaying to $t\bar{t}$ in $p\bar{p}$ Collisions at $\sqrt{s} = 1.8\,\text{TeV}$," Phys. Rev. Lett. 85 (2000) 2062.
[7] DØ Collaboration, V. Abazov et al., "Search for Narrow $t\bar{t}$ Resonances in $p\bar{p}$ Collisions at $\sqrt{s} = 1.8\,\text{TeV}$," Phys. Rev. Lett. 92 (2004) 221801.
[8] CDF Collaboration, T. Aaltonen et al., "Search for resonant $t\bar{t}$ production in $p\bar{p}$ collisions at $\sqrt{s} = 1.96\,\text{TeV}$," `arXiv:0709.0705[hep-ex]`, 2007.
[9] CDF Collaboration, T. Aaltonen, "Limits on the production of narrow $t\bar{t}$ resonances in $p\bar{p}$ collisions at $\sqrt{s} = 1.96\,\text{TeV}$," `arXiv:0710.5335[hep-ex]`, 2007.
[10] D0 Collaboration, V. M. Abazov et al., "Search for $t\bar{t}$ resonances in the lepton+jets final state in $p\bar{p}$ collisions at $\sqrt{s} = 1.96\,\text{TeV}$," DØ Note 5600 conf, 2008.
[11] D0 Collaboration, V. M. Abazov et al., "Search for ttbar resonances in the lepton plus jets final state in ppbar collisions at sqrts=1.96TeV," Phys. Lett. B668 (2008) 98–104.
[12] R. M. Harris, C. T. Hill, and S. Parke, "Cross section for Topcolor Z' decaying to $t\bar{t}$," `hep-ph/9911288`, 1999.
[13] D0 Collaboration, V. M. Abazov et al., "The upgraded D0 detector," Nucl. Instrum. Meth. Phys. Res. A 565 (2006) 463.
[14] D0 Collaboration, S. Abachi et al., "The D0 detector," Nucl. Instrum. Meth. Phys. Res. A 338 (1994) 185.
[15] V. M. Abazov et al., "The muon system of the Run II D0 detector," Nucl. Instrum. Meth. Phys. Res. A 552 (2005) 372.
[16] D0 Collaboration, V. M. Abazov et al., "Measurement of the $t\bar{t}$ production cross section in $p\bar{p}$ collisions at $\sqrt{s} = 1.96\,\text{TeV}$ using kinematic characteristics of lepton + jets events," Phys. Lett. B 626 (2005) 45.
[17] D0 Collaboration, V. M. Abazov et al., "Measurement of the $t\bar{t}$ production cross section in $p\bar{p}$ collisions at $\sqrt{s} = 1.96\,\text{TeV}$ using lepton + jets events with lifetime b-tagging," Phys. Lett. B 626 (2005) 35.
[18] G. Blazey et al., in "QCD and weak boson physics in Run II", U. Baur, R. K. Ellis, and D. Zeppenfeld, Eds., FERMILAB-PUB-00-297, 2000.
[19] T. Scanlon, "*b*-tagging and the search for neutral supersymmetric Higgs bosons at D0," FERMILAB-THESIS-2006-43.
[20] Sjöstrand, Torbjorn and Lönnblad, Leif and Mrenna, Stephen, "PYTHIA 6.2: Physics and manual," `hep-ph/0108264`, 2001.
[21] M. L. Mangano, M. Moretti, F. Piccinini, R. Pittau, and A. D. Polosa, "ALPGEN, a generator for hard multiparton processes in hadronic collisions," JHEP 07 (2003) 001.
[22] S. Höche et al., "Matching parton showers and matrix elements," `hep-ph/0602031`, 2006.
[23] E. E. Boos, V. E. Bunichev, L. V. Dudko, V. I. Savrin, and A. V. Sherstnev, "Method for simulating electroweak top-quark production events in the nlo approximation: Singletop event generator," Phys. Atom. Nucl. 69 (2006) 1317.
[24] D. Stump et al., "Inclusive jet production, parton distributions, and the search for new physics," JHEP 10 (2003) 046.
[25] R. Brun and F. Carminati, CERN Program Library Long Writeup W5013, 1993.
[26] N. Kidonakis and R. Vogt, Eur. Phys. J. C 33 (2004) 466.
[27] Z. Sullivan, "Understanding single-top-quark production and jets at hadron colliders," Phys. Rev. D 70 (2004) 114012.
[28] J. M. Campbell and R. K. Ellis, "An update on vector boson pair production at hadron colliders," Phys. Rev. D 60 (1999) 113006.
[29] T. Andeen et al., "Determination of the effective inelastic $p\bar{p}$ cross-section for the D0 Run II luminosity measurement," FERMILAB-TM-2365, 2007.
[30] S. Moch and P. Uwer, "Theoretical status and prospects for top-quark pair production at hadron colliders," Phys. Rev. D 78 (2008).
[31] Tevatron Electroweak Working Group Collaboration, "Combination of CDF and D0 Results on the Mass of the Top Quark,". arXiv:0808.1089 [hep-ex].
[32] I. Bertram et al., "A recipe for the construction of confidence limits," FERMILAB-TM-2104.